JOURNAL OF MATERIALS SCIENCE 17 (1982) 1610–1616

Electrical conductivity of carbon–polymer composites as a function of carbon content

KEIZO MIYASAKA, KIYOSI WATANABE, EIICHIRO JOJIMA,
HIROMI AIDA, MASAO SUMITA, KINZO ISHIKAWA
Tokyo Institute of Technology, Department of Textile and Polymeric Materials, Ookayama, Meguro-ku, Tokyo, Japan

The electrical conductivity of carbon particle-filled polymers was measured as a function of carbon content to find a break point of the relationships between the carbon content and the conductivity. The conductivity jumps by as much as ten orders of magnitude at the break point. The critical carbon content corresponding to the break point varies depending on the polymer species and tends to increase with the increase in the surface tension of polymer. In order to explain the dependency of the critical carbon content on the polymer species, a simple equation was derived under some assumptions, the most important of which was that when the interfacial excess energy introduced by carbon particles into the polymer matrix reaches a "universal value", Δg^*, the carbon particles begin to coagulate so as to avoid any further increase of the energy and to form networks which facilitate electrical conduction. The equation well explains the dependency through surface tension, as long as the difference of the surface tensions between the carbon particles and the polymer is not very small.

1. Introduction

It has been known that the electrical conductivity of insulating polymers filled with conducting particles, such as metal and carbon powder, discontinuously increases at some content of the filler [1–13]. This sharp break in the relationship between the filler content and the conductivity of composites implies some sudden change in the dispersing state of conducting particles, i.e. the coagulation of particles to form networks which facilitates the electrical conduction through the composites. The same phenomenon has been observed for ceramic composites. For example, Grekila and Tien [14] studied the electrical conductivity of ZrO_2–CaO composites to present a geometrical model for the conductivity in a two-phases system.

The transition-like change in the conductivity of these composites has attracted many researchers to propose models for the phenomenon [2–4, 7–9]. For example, Buche [3] applied Flory's theory for gelation taking place during polymerization of polyfunctional monomers [15] to predict the sharp increase of the electrical conductivity at the particular carbon contents, and Aharoni [4] used an averaged number of contact of conduction particles to discuss the possibility of the network formation. These approaches are all very interesting. We have to point out, however, that the geometrical effects are too much emphasized in their models, while the thermodynamic effects are hardly taken into consideration. This makes it difficult for their models to explain why the break in the conductivity change should depend on the species of polymer and filler, as will be shown later.

In the present paper we first study experimentally the dependency of the critical carbon content corresponding to the break point on the polymer species, and then try to explain the result using a simple model. An excess energy due to the formation of carbon–polymer interfaces plays the most important role in our model. We assume that when the excess energy reaches a "universal" value independent of polymer species, the carbon particles begin to coagulate to form networks in the composite. Some researchers [11, 12] believe that the jump of the electrical conductivity is due

0022–2461/82/061610–07$03.34/0

TABLE I Sample polymers and mixing temperature

Polymer	Details	Mixing temperature (°C)	Film casting temperature (°C)
Linear polyethylene (LPE)	Sholex 5065	150	150
Branched polyethylene (BPE)	Sholex M221	140	140
it.Polypropylene (it.PP)	Ubekosan 109	170	170
Polystylene (PS)	Wako, Dp = 1600 to 1800	150	150
Nylon 6	Teijin, [ ] = 1.34 at 30° C in methacresol	225	225
Polymethylmethacrylate (PMMA)	Mitsubishi Rayon, DP = 4000	20*	210
Natural rubber (NR)		80	148
Stylene-butadiene rubber (SBR)	Nipol 1500	80	148

*Plasticized

to the "tunnel effect" in the thin layers of polymer sandwiched by conducting particles, but not to "passing through network conduction". In the present paper we are not interested in the mechanism of electrical conduction in the composites. It should be, however, noticed that our experiment on the gas sorption by carbon–natural rubber composites showed that the gas-absorptivity of carbon powder markedly decreases near the break point of the electrical conductivity [16]. This reduction of the gas-sorptivity must be due to the decrease in the sorption sites on the surfaces of carbon particles, which has been caused by the coagulation of the particles.

2. Experimental procedure

2.1. Composite sample preparation

Six kinds of polymer listed in Table I and a carbon filler (Seast 300 HAF, 27 nm in diameter) were used in this study. Two kinds of carbon filler were used in additional experiments for discussion of the effects of filler size on the critical carbon content. Each polymer except PMMA was mixed with a given amount of carbon filler in a two-roller mill for 20 minutes at temperatures shown in Table I. Prior to the mixing, both the polymers and the carbon filler were dried at 80° C for 24 h under vacuum. A longer mixing time is effective in making the mixture uniform, whilst a shorter time must be favoured to avoid polymer degradation which is more or less necessarily caused by the mechanical action of the roller mill. The condition for the mixing shown above was chosen by taking these reasons into consideration. The fact that the samples thus prepared gave highly reproducible data on the conductivity implied that the almost equilibrium mixed state was achieved in them. PMMA was too viscous to mix with carbon even at temperatures much higher than the glass transition point, (mixing above 250° C was difficult in our mill). Thus the polymer was plasticized with a small amout of acetone and then mixed with carbon in the roller mill. After mixing, the acetone was removed from the mixture under vacuum. These procedures for PMMA mixing were performed at room temperature. Films 1 mm thick were prepared from the polymer–carbon mixtures, inclusive of PMMA mixture, by heat-casting followed by quenching into ice water. The temperature of the casting was the same as that of mixing as shown in Table I, with an exception of PMMA. In addition to the composite samples from 6 kinds of polymer, carbon–rubber composites from natural rubber and SBR (23.5% styrene, 76.2% butadiene) were used. These rubber samples were filled with the same carbon as that for the other polymers. However, they also contained small amount of agents such as zinc oxide, stearic acid, sulphur and softner (aromatic oil). These impurities must affect the electrical conduction of the sample, and therefore the data obtained on these rubber samples were only taken for reference.

2.2. Electrical conduction measurements

The electrical conductivity was measured in the thickness direction of the composite films. Silver paste was used to ensure good contact of the sample surface with the electrodes of the conduction tester. The electrical conductivity of the samples varied over a wide range from 10^{-18} to $1\ \Omega^{-1}\ \mathrm{cm}^{-1}$. Low conductivity samples were measured under $2.5\ \mathrm{kV\ cm}^{-1}$ and $5.5\ \mathrm{kV\ cm}^{-1}$ using a Takedariken TR-84M vibrating reed electrometer, while high conductivity samples were measured under $10\ \mathrm{V\ cm}^{-1}$ and $15\ \mathrm{V\ cm}^{-1}$ using a Sanwa EM1000 universal tester. Prior to the measurements, all the samples were kept in a desi-

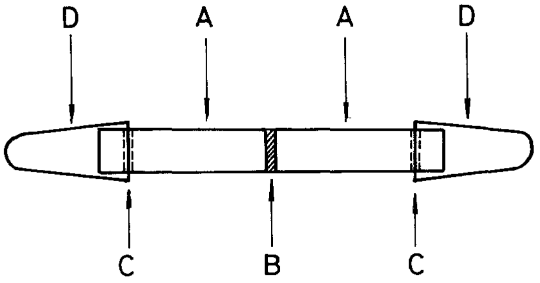

Figure 1 Schematic drawing of a test piece for adhesion strength measurement, showing A, carbon rod; B, joined part with polymer; C, hole for D to pass through and D, steel string to be cramped by jaws of extensometer.

cator with P_2O_5, and the conductivity was measured in dry air at 20° C.

2.3. Adhesion test

Test pieces whose schematic drawing is shown in Fig. 1 were prepared to measure the adhesion force. Carbon rods 3 cm long and 8 mm in diameter which were originally electrodes of a dry cell were joined with the polymer melt at nearly the same temperatures as the mixing in the composite sample preparation, and then cooled in the atmosphere at room temperature. Then the excess polymer, which overflowed from the joined part, was removed by use of a razor. The test pieces were stretched at a rate of 4 mm min^{-1} at room temperature in an Instron type extensometer. Adhesion strength was defined as the breaking stress standardized by the sectional area of the carbon rod. The adhesion test was not done for NR and SBR because of the difficulty in the sample preparation.

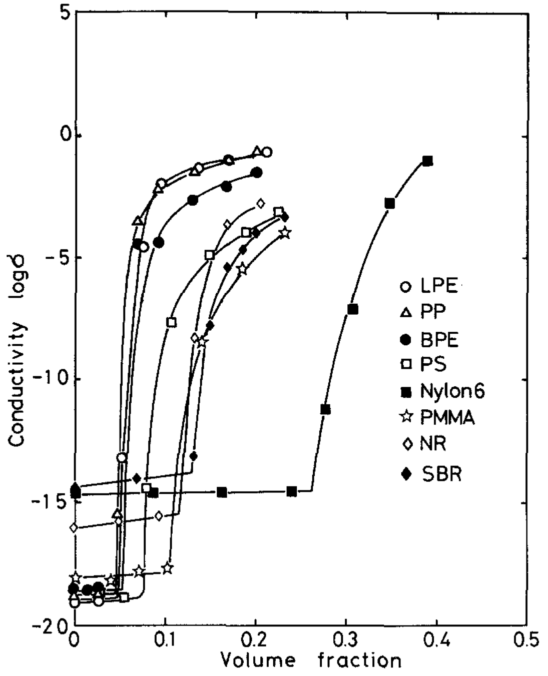

Figure 2 Electrical conductivity of polymer composites filled with carbon particles as a function of carbon content. (σ is in Ω^{-1} cm^{-2}).

3. Results and discussion

Fig. 2 shows the electrical conductivity of the composite films as a function of volume fraction of carbon filler. At zero content (pure polymer), the conductivity varies widely: The high conductivity of nylon 6 is due to the amide group, and that of NR and SBR is due to the conjugated double bonds and to the agents added in the sample preparation. The change in the conductivity of all the samples with carbon addition is not monotonic: whilst the carbon content remains less than a value which seems to be characteristic to each polymer, the change is slight and continuous. The conductivity, however, jumps as high as 10 orders of magnitude when the carbon content reaches a particular value. After the transition-like increase, the change of conductivity again becomes mild as before. This jump of conductivity indicates that some drastic change occurs in the state of dispersion of carbon particles in polymer matrix, i.e. the beginning of coagulation resulting in networks facilitating the electrical conduction. The critical carbon content corresponding to the conductivity jump varies from 4.7 vol% for it.PP to 27.0 vol% for nylon 6, suggesting that the polarity of polymer may relate to the critical content: The higher the polarity of a given polymer, the larger the critical content is. This makes us expect that the critical content must depend on the surface tension of polymer. and therefore the content is plotted against the tension in Fig. 3. The values of the tension were from [17] for 6 kinds of polymers, and from [18] for NR. Fig. 3 shows that the content is related to the surface tension of polymer, with exceptions for it.PP and NR. The data for SBR is not plotted in the figure, because the value of the surface tension was not available. It may be reasonable to consider that the impurities other than carbon particles added in the sample preparation increases the affinity of rubber to carbon filler. This made us assume that the deviation of plots for rubber composite observed in Fig. 3 is due to the underestimation of the surface tension. Then we can

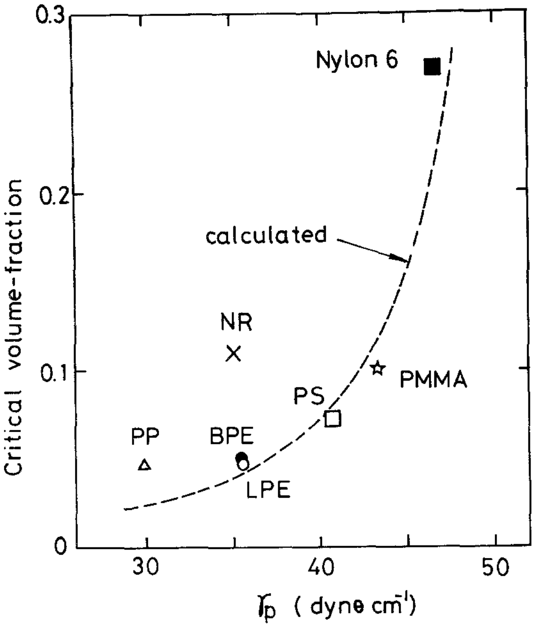

Figure 3 Plot of the critical carbon content against the surface tension of polymer. The dotted line shows the best-fit curve calculated by Equation 11 with values of c and Δg^* shown in the text.

recognize a correlation between the surface tension of the polymer and the critical carbon content: The larger the surface tension, the larger the critical content is.

In Fig. 4 the critical carbon content is plotted against the adhesion strength to show that there is a correlation between them: The larger the adhesion strength of the polymer, the larger the critical carbon content. This indicates that the adhesion strength also depends on the affinity of polymer to carbon particles.

The results obtained above led us to conclude that the critical carbon content must be related with the excess energy produced in the polymer–carbon interface. We try to explain the relationship between the critical carbon content and the surface tension shown in Fig. 3, on the basis of the interfacial energy. In a carbon-filled composite sample the volume fraction, V_f, of carbon is defined by

$$V_f = NV_0/(1 + NV_0), \tag{1}$$

where N is the number of carbon particles per unit volume of polymer, and V_0 is the volume of a carbon particle. The addition of carbon to a polymer necessarily produces a polymer–carbon interface. Let Δg, the interfacial excess energy produced in a unit volume of polymer, be expressed by

$$\Delta g = K[S], \tag{2}$$

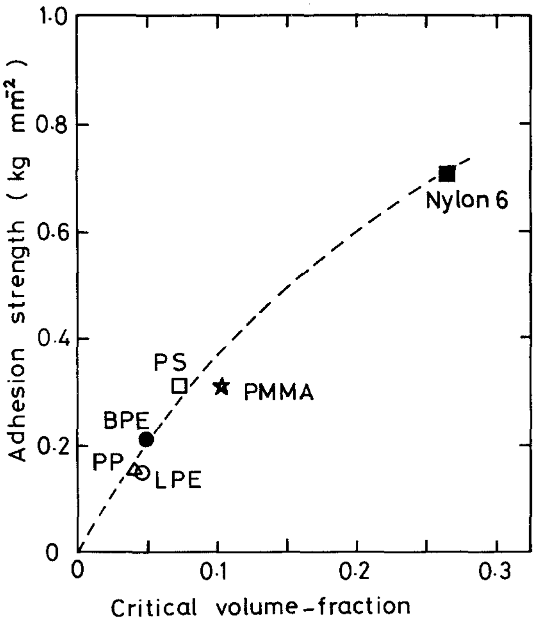

Figure 4 Plot of the critical carbon content against the adhesion strength of polymer.

where $[S]$ is the total area of the interfaces per unit volume of polymer and K is the interfacial energy per unit area of the interface. We only consider the case where K is positive, and therefore Δg is positive. $[S]$ is expressed by

$$[S] = PNS_0, \tag{3}$$

where S_0 is the surface area of a carbon particle, and P is a parameter indicating the state of dispersion of carbon particles: When all the particles disperse isolated from others, P is equal to unity, and it decreases with coagulation of particles. Thus

$$\Delta g = KPNS_0. \tag{4}$$

We make following assumptions:

Assumption 1. Carbon particles begin to coagulate only when Δg reaches Δg^*, i.e., a particular value of the excess energy. This means that P is kept at unity before Δg reaches Δg^*. Fig. 5 shows the meaning of this assumption. Therefore

$$\Delta g = KNS_0 \qquad \text{for } \Delta g < \Delta g^* \tag{5}$$

and

$$\Delta g^* = KN^*S_0 \qquad \text{at the critical point} \tag{6}$$

where the critical point is that where Δg reaches Δg^*, and N^* is the number of carbon at the critical point.

Assumption 2. The value of Δg^* is a universal constant independent of polymer species. This

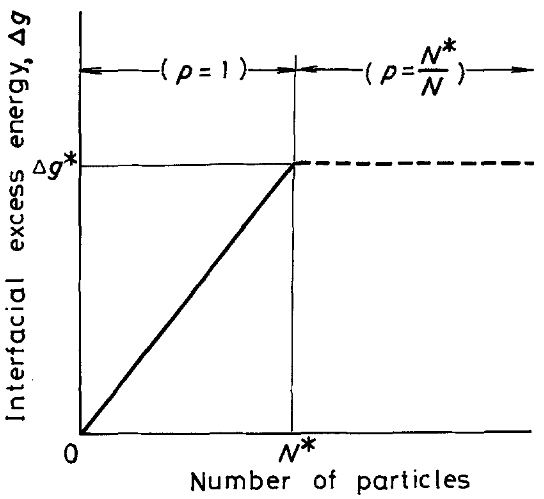

Figure 5 Schematic representation of assumed relation between the interfacial excess energy and number of carbon particle. For $V_f < V_f^*$, the slope is constant depending on K and S_0, and it becomes zero for $V_f > V_f^*$.

together with Assumption 1 mean that carbon particles begin to coagulate at an iso-interfacial energy state of the polymer which is the expression analagous to the iso-free volume state for the glass transition point [19].

Replacing N in Equation 1 by N^* in Equation 6 gives Equation 7 to the critical volume fraction.

$$V_f^* = [1 + (K/\Delta g^*)(S_0/V_0)]^{-1}. \qquad (7)$$

For spherical particles,

$$(S_0/V_0) = 3/R. \qquad (8)$$

As Δg^* has been assumed to be a universal constant, V_f^* is a function of (S_0/V_0) determined by the geometry of filler and of K, the interfacial energy depending on the polymer species. Then an assumption is made for K.

Assumption 3. K is given by Equation 9 proposed by Fowkes [20].

$$K = \gamma_c + \gamma_p - 2(\gamma_c \gamma_p)^{1/2} \qquad (9)$$

where γ_c and γ_p are the surface tensions of carbon particles and polymer respectively. It is well known that this relation is only reasonable for non-polar systems in which the surface tension is due to dispersion force. A relationship which is applicable to general systems inclusive of polar contribution, has been studied. For example, Hata and Kitazaki [17] proposed an equation for the interfactial energy which consists of nonpolar, polar and hydrogen bonding contributions, under assumption that the Fowkes's relation (Equation 9) was applicable to each of the three contributions. It might be better to use their equation than to use Equation 9 for general systems including polar contributions. Nevertheless we make Assumption 3 at this time, because we are concerned at the validity of the assumptions made in their equation, and also of the complication which would be caused by use of their equation. We must, however, recognize that Assumption 3, the use of Equation 9 for general systems including polar contributions, is so rough that it might have made our theoretical approach "technological" rather than "scientific". Substitution of Equation 9 into Equation 7 gives

$$V_f^* = [1 + (\gamma_c^{1/2} - \gamma_p^{1/2})^2 (S_0/V_0)/\Delta g^*]^{-1}. \qquad (10)$$

This reduces into Equation 11 for spherical particles.

$$V_f^* = [1 + 3(\gamma_c^{1/2} - \gamma_p^{1/2})^2/(\Delta g^* R]^{-1} \qquad (11)$$

In these equations V_f^* is a unique function of γ_p, the surface tension of a given polymer, when carbon particles of the same size and quality are used, because of the constant γ_c and (S_0/V_0) or R.

The critical content values, V_f^*, obtained above were analysed by Equation 11: Simultaneous equations which were a function of Δg^* and γ_c were made by substituting the experimental values of V_f^* and γ_p from literature and 27 nm for R into Equation 11. The calculation of the equations showed that 5.5×10^{-2} N m^{-1} for γ_c and 2.1×10^5 J m^{-3} for Δg^* gave the best fit between observed and calculated $\gamma_p - V_f^*$ relation. The dotted line in Fig. 3 shows the relation of Equation 11 with these constants for γ_c and Δg^*. It may be reasonable to consider that the state of particle dispersion is determined during mixing or film casting. This means that γ_p in the above equations should be that at mixing or film casting temperature. We, however, used the values at room temperature, for no data at high temperature were available. The dotted line in Fig. 3 seem to explain satisfactorily the experimental $\gamma_p - V_f^*$ relation, if the deviations for it.PP and rubbers would be caused by the underestimation of γ_p values, as mentioned above.

Equations 11 and 10 expect that the value of V_f^* increases with the increase in R the diameter of spherical particles, or in (V_0/S_0) the ratio of volume to the surface area of particles of any shape. In order to examine the validity of the equations, the effect of R on the value of V_f^* was studied for HDPE, LDPE, PS and nylon 6, using 41 nm and 56 nm carbon particles additionally to 27 nm particle which has been used so far. The jump of the electrical conductivity was observed in all these samples, and the V_f^* was estimated for each polymer as a function of the particle diameter. On the other hand, the V_f^* values for these fillers were calculated by Equation 11 with the same constants as those determined above for 27 nm particle, as a function of the diameter. Both calculated and observed values of V_f^* are plotted against the diameter of carbon particle in Fig. 6 with the exception that only the observed values are shown for 27 nm particles. The calculated values for the 27 nm particles are necessarily equal to the observed values, for the constants in Equation 11 have been chosen for 27 nm data. The observed V_f^* values increase with increasing diameter of the carbon particles, as is expected from Equation 11, and the difference between the observed and calculated V_f^* values is not large. This seems to indicate that the equation for V_f^* drived above may be valid for these non-polar polymers with comparatively small surface tension. On the other hand, the following values of V_f^* were obtained for nylon 6: 0.264 for the 27 nm particle, 0.20 for the 41 nm particle and 0.22 for the 56 nm particle. It is difficult to find any systematic change of V_f^* with particle size in this case, which seems to imply that the equation might not be valid. However, we have to think of the property of these equations relating to the value of γ_c. They indicate that when the difference between the values of γ_c and γ_p is small, as is the case for nylon 6, even a small change in γ_c value causes a large change in the value of V_f^*. This means that the application of the equations to the case where the value of γ_p is close to that of γ_c should be avoided. It may be reasonable to assume that the three carbon particles different in their size were different also in their surface energy more ~~of~~ less, and that this is the reason why no systematic change in the V_f^* value with the change in the particle size was observed in the case of nylon 6.

Our interest has been so far concentrated on the critical point at which carbon particles would begin to coagulate. We now consider what would happen after the critical point. It may be reasonable to consider that the Assumption 1 implies that the interfacial energy would be kept at Δg^* in the composite polymers filled with more carbon than V_f^*, as schematically shown by the dotted line in Fig. 5. Therefore

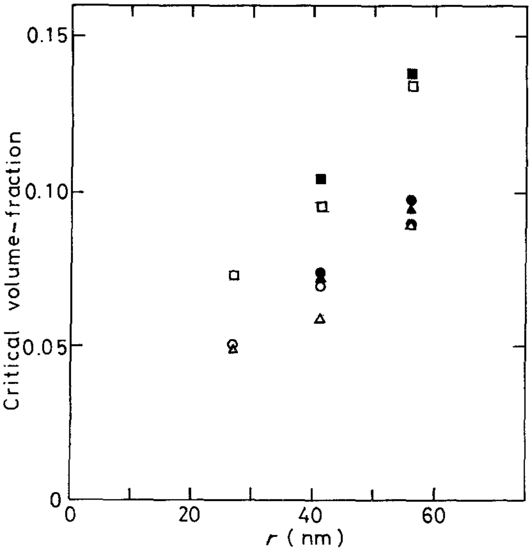

Figure 6 Critical carbon content as a function of the diameter of the carbon particles. (□, Pst(obs); ■, Pst(cal); △, LPE(obs); ▲, LPE(cal); ○, BPE(obs), and ●, BPE (cal)).

$$\Delta g^* = KPNS_0$$

or

$$PN = N^* \qquad \text{for } N > N^* \tag{12}$$

In this expression Δg^* is the upper limit of the interfacial energy which all the polymers can have commonly. Equation 12 expects that the coagulation is accelerated with the carbon content beyond the critical point, which explains the reason why the critical point is followed by such a transition-like large increase of the conductivity as seen in Fig. 2.

Acknowledgements

The authors wish to express their gratidude to Dr Hirakawa and Dr Mizoguchi of the Research Institute of Hokohama Rubber Co. for their kindness in providing NR and SBR samples.

References

1. J. GARLAND, *Trans. Met. Soc. AIME* **236** (1966) 642.
2. A. MALLIARIS and D. T. TURNER, *J. Appl. Phys.* **42** (1972) 614.
3. F. BUCHE, *ibid.* **43** (1972) 4837.
4. S. M. AHARONI, *ibid.* **43** (1972) 2463.
5. R. P. KUSY and D. T. TURNER, *J. Appl. Polymer Sci.* **17** (1973) 1631.

6. F. BUCHE, *J. Appl. Phys.* **44** (1973) 532.
7. R. M. SACRISBRICK, *J. Phys. D.* **6** (1973) 2098.
8. G. E. PIKE and C. H. SEAGER, *Phys. Rev. B,* **10** (1974) 1421.
9. C. H. SEAGER and G. E. PIKE, *ibid.* **10** (1974) 1435.
10. R. MUKHOPADHYAY, S. K. DE and S. BASU, *J. Appl. Polymer Sci.* **20** (1976) 2575.
11. W. F. VERHELST, K. G. WOLTHUIS, A. VOET, P. EHRBURGER and J. B. DONNET, *Rubber Chem. Tech.* **50** (1977) 735.
12. A. K. SIRCAR and T. G. LAMOND, *ibid.* **51** (1978) 126.
13. R. MATSUSHITA, M. SENNA and H. KUNO, *J. Mater. Sci.* **12** (1977). 509.
14. R. B. GREKILA and T. Y. TIEN, *J. Amer. Ceram. Soc.* **48** (1965) 22.
15. P. J. FLORY, "Principles of Polymer Chemistry", (Cornell University Press, 1953) Chapter 9.
16. A. TANIOKA, K. MIYASAKA and K. ISHIKAWA, *J. Polymer. Sci., Polymer. Phys. Ed.* to be published.
17. Y. KITAZAKI and T. HATA, *J. Adhesion Soc. Japan,* **8** (1973) 131.
18. K. L. JOHNSON, K. KENDALL and A. D. ROBERT , *Proc. Roy. Soc. London* **324** (1971) 301.
19. M. L. WILLIAMS, R. F. LANDEL and J. FERRY, *J. Amer. Chem. Soc.* 77 (1955) 3701.
20. F. M. FOWKES, *Ind. Eng. Chem.* **56** (1964) 40.

Received 18 November 1980
and accepted 4 November 1981